Few-Body Systems 30, 95–120 (2001)

Few-Body Systems

© Springer-Verlag 2001
Printed in Austria

Novel Three-Nucleon-Force Terms in the Three-Nucleon System*

D. Hüber[1,2,**], J. L. Friar[1], A. Nogga[3], H. Witała[4], and U. van Kolck[5]

[1] Theoretical Division, Los Alamos National Laboratory, M.S. B283, Los Alamos, NM 87545, USA
[2] living systems AG, Humboldtstraße 11, D-78166 Donaueschingen, Germany
[3] Institut für Theoretische Physik II, Ruhr-Universität Bochum, D-44780 Bochum, Germany
[4] Institute of Physics, Jagellonian University, PL-30059 Cracow, Poland
[5] Kellogg Radiation Laboratory, 106-38, California Institute of Technology, Pasadena, CA 91125, USA

Abstract. We include two specific three-nucleon-force terms of pion-range–short-range form in our momentum-space calculations for the three-nucleon continuum. These two terms are expected by chiral perturbation theory to be non-negligible. We study the effects of these terms in elastic neutron-deuteron scattering and pay special attention to the neutron vector-analyzing power A_y.

1 Introduction

Recently it became possible to explain differences between data and predictions of modern nucleon-nucleon (*NN*) potentials for the total neutron-deuteron (*nd*) cross section and the minimum of the differential *nd* cross section at higher energies by incorporating the 2π-exchange Tucson-Melbourne (TM) three-nucleon force (3NF) [1, 2]. However, the puzzling discrepancy between theory and data for the low-energy analyzing power [3] cannot be explained by that 3NF. Since it was shown in ref. [4] that this low-energy analyzing-power puzzle cannot be solved by reasonable changes in the *NN* potentials, one obviously needs new 3NF mechanisms in order to resolve this long-standing mystery.

The number of possible operators that can be used in constructing a 3NF is much larger than in the *NN*-force case, and it is not practicable to examine them all in order to see which are important for the low-energy analyzing powers and which are not. Rather, we need a systematic scheme that tells us which terms are likely candidates to be of importance and which are not. One such approach is chiral perturbation theory (χPT), which provides a power-counting scheme for the strength of the various 3NF terms.

* Dedicated to Prof. W. Glöckle on the occasion of his 60th birthday

** E-mail: dirk.hueber@living-systems.de

As we will explain below, χPT predicts in lowest non-vanishing order (beside the usual 2π-exchange terms) two terms of pion-range–short-range nature and three terms of short-range–short-range nature. Short range means, for example, that a meson heavier than a pion is exchanged between two of the three nucleons. Since the naive expectation is that pion-range–short-range 3NF terms are more important than the ones of short-range–short-range nature, in this paper we will deal only with the two pion-range–short-range 3NF terms, which we will include in our momentum-space calculations for the 3N continuum. Our interest will be concentrated on the low-energy vector-analyzing powers.

In Sect. 2 we review the history of the 2π-exchange 3NF and its effect in the 3N continuum. In Sect. 3 we discuss those 3NF terms that include the exchange of mesons heavier than pions and that have been tested in the 3N continuum thus far.

The two 3NF terms of pion-range–zero-range nature that are predicted in lowest non-vanishing order of χPT are introduced in Sect. 4. In this section we also explain how we adapt these terms, making them of finite range in order to be consistent with the traditional potentials that we use as our *NN* force, and also with the TM force that we use as our 2π-exchange 3NF in this paper. At the end of this section we discuss what conventional nuclear field-theory models say about these two 3NF terms.

Our approach to solving the Faddeev equations for the $3N$ continuum is reviewed briefly in Sect. 5.

The results for the *nd* elastic-scattering observables that incorporate the new 3NF terms are presented and discussed in Sect. 6.

Finally we sum up and conclude in Sect. 7.

In Appendix A, we present the partial-wave decomposition (PWD) for the two new 3NF terms.

2 Short Review of 2π-Exchange Three-Nucleon Forces

Three-nucleon forces have been part of nuclear physics for more than 40 years. Realistic models began with the Fujita-Miyazawa (FM) force [5], which describes the exchange of two pions with an intermediate Δ-isobar as depicted in Fig. 1. Fig. 1 shows only that part of the 3NF for which nucleon 1 is the middle nucleon (i.e., the nucleon at which the virtual pion scattering takes place). We will call this configuration $V_4^{(1)}$ [1]. The full 3NF is then given by

$$V_4 = V_4^{(1)} + V_4^{(2)} + V_4^{(3)}. \tag{1}$$

Scattering the pion in Fig. 1 from nucleon 1 via a virtual Δ-isobar is not the most general process that leads to a 2π-exchange 3NF. The many ways to accomplish this are indicated by the blob in Fig. 2. Several ansätze have been used to derive the 2π-exchange 3NF up to now. A short overview is given in Table 1. We will not comment here on the different techniques and the underlying physical ideas that lead to these 3NF models. For that we refer the interested reader to our recent paper [11]. Rather, we will concentrate here on the differences between

[1] The use of the index "4" for a 3NF is common usage for three-nucleon calculations, where the indices "1"–"3" denote the three *NN*-pair forces

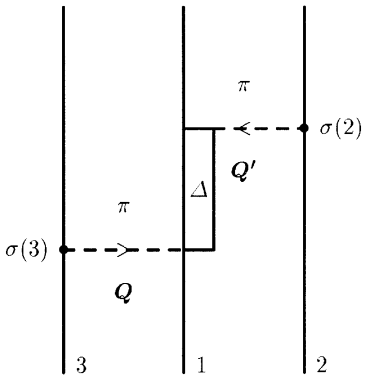

Fig. 1. The Fujita-Miyazawa 3NF

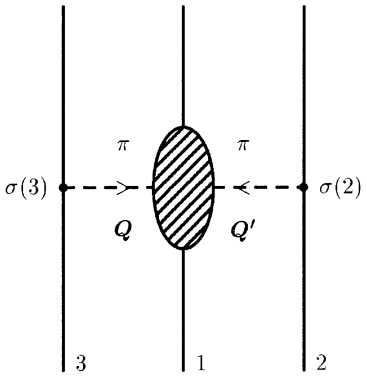

Fig. 2. The 2π-exchange 3NF

Table 1. Various 2π-exchange 3NF models in use today

Year	3NF	Characteristic	a'	b	c	d
1957	Fujita-Miyazawa [5]	Isobars	0	−1.15	0	−0.29
1979	Tucson-Melbourne [6]	Current algebra	−1.03	−2.62	1.03	−0.60
1983	Brazil [7]	Chiral Lagrangean + (current algebra)	−1.05	−2.29	(1.05)	−0.77
1983	Urbana [8]	Isobars with additional phenomenological medium-range term	0	−1.20	0	−0.30
1993	Texas [9]	Chiral perturbation theory	−1.87	−3.82	0	−1.12
1996	RuhrPot [10]	Non-chiral Lagrangean	−0.51	−1.82	0	−0.48

these models in terms of operator form and the effects of these different models in $3N$ calculations.

Let us begin with the types of operators contained in various 3NF models in use today. We will use the familiar language of the Tucson-Melbourne force [6], which labels four 2π-exchange operators by its parameters a, b, c, and d. The operator form of these terms (neglecting all overall factors and form factors) is given by

$$V_4^{(1)}|_a = \frac{1}{\boldsymbol{Q}^2 + m_\pi^2} \; \frac{1}{\boldsymbol{Q}'^{\,2} + m_\pi^2} \; \boldsymbol{\tau}_2 \cdot \boldsymbol{\tau}_3, \tag{2}$$

$$V_4^{(1)}|_b = \frac{1}{\boldsymbol{Q}^2 + m_\pi^2} \frac{1}{\boldsymbol{Q}'^2 + m_\pi^2} \boldsymbol{Q} \cdot \boldsymbol{Q}' \, \boldsymbol{\tau}_2 \cdot \boldsymbol{\tau}_3, \tag{3}$$

$$V_4^{(1)}|_c = \frac{1}{\boldsymbol{Q}^2 + m_\pi^2} \frac{1}{\boldsymbol{Q}'^2 + m_\pi^2} (\boldsymbol{Q}^2 + \boldsymbol{Q}'^2) \, \boldsymbol{\tau}_2 \cdot \boldsymbol{\tau}_3, \tag{4}$$

$$V_4^{(1)}|_d = \frac{1}{\boldsymbol{Q}^2 + m_\pi^2} \frac{1}{\boldsymbol{Q}'^2 + m_\pi^2} \boldsymbol{\sigma}_1 \cdot \boldsymbol{Q} \times \boldsymbol{Q}' \, \boldsymbol{\tau}_1 \cdot \boldsymbol{\tau}_2 \times \boldsymbol{\tau}_3, \tag{5}$$

where we have used the notation implicit in Figs. 1 and 2.

The main difference between all these models (in terms of operator structure) is the c-term in the TM force. Let us have a closer look at the c-term and rewrite it (neglecting the isospin dependence in Eq. (4)) as

$$\begin{aligned} V_4^{(1)}|_c &\propto \frac{\boldsymbol{Q}^2}{\boldsymbol{Q}^2 + m_\pi^2} \frac{1}{\boldsymbol{Q}'^2 + m_\pi^2} + (Q \leftrightarrow Q') \\ &= \frac{\boldsymbol{Q}^2 + m_\pi^2 - m_\pi^2}{\boldsymbol{Q}^2 + m_\pi^2} \frac{1}{\boldsymbol{Q}'^2 + m_\pi^2} + (Q \leftrightarrow Q') \\ &= \left(\underbrace{1}_{\text{SR}} - \underbrace{\frac{m_\pi^2}{\boldsymbol{Q}^2 + m_\pi^2}}_{\pi\text{-range}} \right) \frac{1}{\boldsymbol{Q}'^2 + m_\pi^2} + (Q \leftrightarrow Q'). \end{aligned} \tag{6}$$

Thus the c-term can be decomposed into a 2π-exchange term with the same operator structure as the a-term plus a short-range–π-range term (marked ''SR'' in Eq. (6)). The inclusion of the 2π-exchange part of the c-term leads to a redefinition of a as

$$a' = a - 2 \, m_\pi^2 \, c, \tag{7}$$

which essentially means a change of sign for a: $a' \approx -a$. Therefore the difference between the TM model and the other 2π-exchange 3NFs is the former's short-range–π-range part of the c-term. Arguments developed in ref. [11] using chiral symmetry show that this short-range–π-range part of the c-term should be dropped. Doing this (and accordingly replacing a by a'), one gets a ''corrected'' TM force that we will call TM$'$ in what follows.

Since the FM force has included only the 2π-Δ mechanism, it has only the b- and d-terms. Also, for the same reason, the values of b and d are roughly half the size of the corresponding TM-model values.

The Brazil force [7] is very closely related to the TM model; however, it does not have the c-term. (That is, in its original form, although a c-term was later included in order to agree with the TM model; this is indicated by the brackets in Table 1.) The values for the parameters a', b, and d are very close to the TM values.

The Urbana model [8] has only the b- and d-terms with values for b and d like those of the FM model, since it also incorporates only the Δ-mechanism. In addition it has a phenomenological medium-range term, whose inclusion was motivated by nuclear-matter calculations. It turns out that this term plays no important role in the $3N$ system.

Like the Brazil force the Texas force [9] has the a-, b-, and d-terms, but with values for a', b, and d obtained from a fit to π-N scattering and substantially larger than those used in the Brazil or TM models.

Finally, the RuhrPot model [10] also employs the a'-, b-, and d-terms, but with significantly smaller values for the parameters than those used in the TM force.

Consequently one does not expect major differences in the effects of these 2π-exchange 3NFs in the $3N$ system and, indeed, no major differences have been found; (except for the Texas force) all of the above-mentioned 2π-exchange 3NF models have been tested in $3N$ bound-state and continuum calculations, either by the Bochum-Cracow group or the Pisa group or by both. Even the original TM force with the c-term gives results similar to all the other models at low energies, for reasons explained below. The only differences to be found are related to the different strengths of these models due to different values for the parameters, as well as due to different choices for the πNN form factors.

Let us now study the effects of the different terms individually. For the triton this has already been done in ref. [12]. There it was found that the largest contribution to the binding energy (60%–70%) comes from the b-term, whereas the a'-term can be neglected. The rest comes from the c- and d-terms, where the relative importance of these two terms depends strongly on the chosen NN interaction (ref. [12] used the RSC and AV14 potentials).

In order to get the experimental value of the triton binding energy in conjunction with various NN-force models, one can adjust the cut-off parameter Λ in the πNN form factors of the TM and Brazil forces [13]. The πNN form factors of these models have the form

$$F(Q^2) = \frac{\Lambda^2 - m_\pi^2}{\Lambda^2 + Q^2}. \tag{8}$$

Not only does the denominator in Eq. (8) suppress momenta large compared to the cut-off parameter Λ, but because F is normalized to one at $Q^2 = -m_\pi^2$, the numerator (and thus F at low momenta) also varies with Λ. This form factor therefore acts to a certain degree like a strength factor of the 3NF, which allows one to adjust the value of the triton binding energy.

The different versions of the Urbana 3NF are fitted to give the correct value for the triton binding energy when used with one of the Argonne NN potentials.

Most remarkable is the RuhrPot model, because the RuhrPot 2π-exchange 3NF (together with the RuhrPot NN force) gives essentially the experimental value for the triton binding energy without having any adjustable parameters [14].

For the $3N$ continuum we have studied the effects of the individual 3NF terms (a', b, d), in conjunction with the AV18 np potential [15], on elastic-scattering observables at $E_{\rm lab} = 3$ MeV. The result is that the most important role in the 2π-exchange 3NF is played by the b-term. The other terms may have significant contributions to some (small) observables, but they are always smaller than the b-term contribution. As typical examples we depict the vector spin-correlation coefficient C_{xx} and the nucleon-to-deuteron tensor spin-transfer coefficient $K_y^{x'z'}$ in Fig. 3.

This dominance of the b-term explains why all 2π-exchange 3NFs, including the TM force with the c-term, give essentially the same results for the 3N

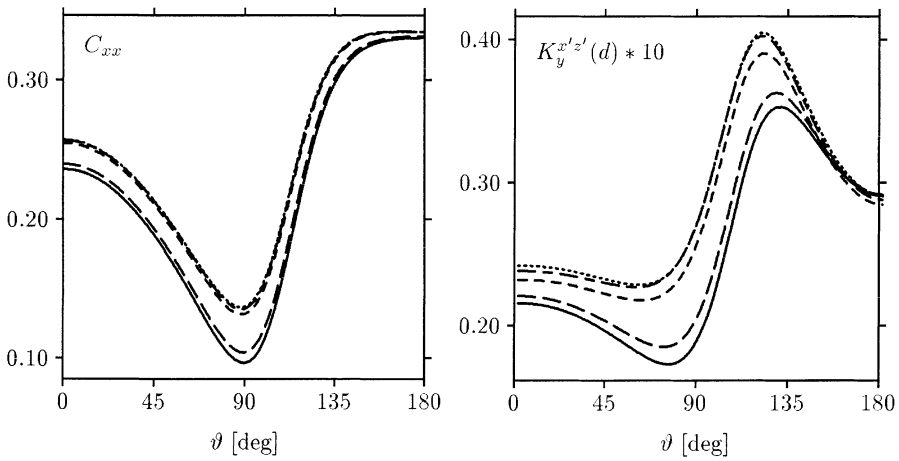

Fig. 3. Effects of the various terms of the TM 2π-exchange 3NF on the vector spin-correlation coefficient C_{xx} and the nucleon-to-deuteron tensor spin-transfer coefficient $K_y^{x'z'}$ at $E_{\rm lab} = 3$ MeV. Predictions are: AV18 (solid line), AV18 + b (short-dashed line), AV18 + d (long-dashed line), AV18 + *abd* (dotted line) and AV18 + *abcd* (long-short dashed line). The 3NFs are switched on only in the $J^\Pi = \frac{1}{2}^\pm$ channels with $j_{\rm max} = 2$

continuum after being fitted to the triton binding energy, even for those observables that do not scale with the triton binding energy. Of course, this picture might change if we go to higher energies.

Interesting within this context is that many low-energy observables, especially in elastic scattering, show the just-mentioned scaling behaviour with the triton binding energy [3] (i.e., all predictions for these observables using Hamiltonians with different *NN* potentials and a 3NF fitted to the triton binding energy agree with each other). We had a closer look at this scaling phenomenon and found (not

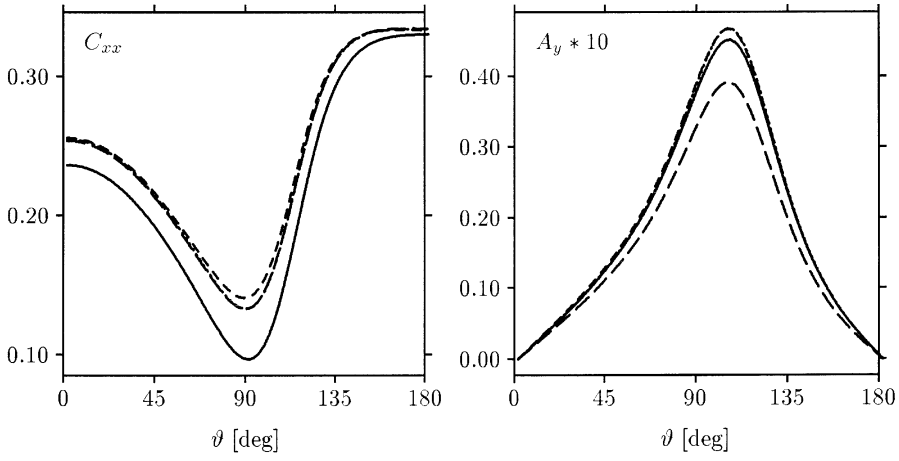

Fig. 4. Contributions of the TM 3NF in various channels for the scaling observable C_{xx} and the non-scaling observable A_y. The prediction without 3NF is the solid line (AV18 only). The TM 3NF is switched on for $J^\Pi = \frac{1}{2}^+$ (short-dashed line), $J^\Pi = \frac{1}{2}^\pm$ (long-dashed line), and $J^\Pi \leq \frac{5}{2}^\pm$ (dotted line), respectively

unexpectedly) that the scaling observables are those that show a nonnegligible 3NF effect *only* in $J^\Pi = \frac{1}{2}^+$ (J being the total three-body angular momentum and Π the parity), whereas non-scaling observables show 3NF effects also (or only) for other values of J^Π. As typical examples we show C_{xx} and A_y in Fig. 4.

3 Three-Nucleon Forces Including Heavier Mesons

The TM model was extended to incorporate the exchange of ρ-mesons in ref. [16], which leads to a π-ρ and a ρ-ρ 3NF [17]. These forces were studied together with the TM π-π 3NF in the $3N$ elastic scattering and breakup process [18].

The result of this study was that the ρ-ρ 3NF has no visible effects, whereas the π-ρ 3NF always has an effect opposite in sign to the effect of the π-π 3NF, but smaller. Moreover, it appears that the effect of the π-ρ 3NF is more or less proportional to the effect of the π-π 3NF.

That result is somewhat surprising. It means that replacing a π with a ρ in the 3NF produces the same effects, though smaller and in the opposite direction. In other words, the effective physics in the π-ρ 3NF is roughly the same as in the π-π 3NF. Given that the ρ and the π interact very differently, this is a surprising conclusion.

In order to understand this let us recall that the most important term in a π-π 3NF is the b-term. If we examine the operator structure of the π-ρ 3NF (see, for example, the last paper of ref. [17]), we find that this force also contains a term with the same operator structure as the b-term of the π-π-exchange TM 3NF, but with different parameters and form factors and with the π-mass in one of the meson propagators replaced by the ρ-mass. Moreover, we find that the π-ρ b-term has the opposite sign to the π-π b-term. So it seems plausible that the TM π-ρ 3NF could be dominated by its b-term, also; at least, that would explain the pattern found in the $3N$ scattering observables. (As a side remark, we note that the π-ρ 3NF also has a d-term, which has the same sign as the π-π d-term.)

Whether our supposition about the π-ρ b-term is true or not, the finding in ref. [18] about the effect of the π-ρ TM 3NF on $3N$ scattering observables shows that the π-ρ 3NF of ref. [17] cannot be expected to contribute to the explanation of any discrepancies between experiment and theory like the A_y-puzzle. This π-ρ 3NF just weakens the π-π 3NF, but does not lead to any new effects. In order to explain current puzzles we need new 3NF terms coming from other physics.

4 The Texas Force and the Texas-Los Alamos Three-Nucleon Force

In addition to the conventional 2π-exchange 3NF terms (the a'-, b-, and d-terms in the TM language), χPT in first non-vanishing order predicts two terms of π-range–zero-range nature (called d_1- and d_2-terms in the language of the Texas force) and three terms of zero-range–zero-range nature (called e_1-, e_2-, and e_3-terms) [9]. Since the zero-range–zero-range terms may be less important than the π-range–zero-range terms (as the ρ-ρ terms in the TM force are much less important than the π-ρ terms), we discuss here only the π-range–zero-range terms, and defer until later the purely short-range terms. The form of the former terms in momentum

space is given by

$$V_4^{(1)} = \frac{d_1}{(2\pi)^6}\,\frac{g_A}{2f_\pi^2}\;\boldsymbol{\sigma}_1\cdot\boldsymbol{Q}'\;\;\boldsymbol{\sigma}_2\cdot\boldsymbol{Q}'\;\frac{1}{Q'^2+m_\pi^2}\;\boldsymbol{\tau}_1\cdot\boldsymbol{\tau}_2 + \frac{d_1}{(2\pi)^6}\,\frac{g_A}{2f_\pi^2}\;\boldsymbol{\sigma}_1\cdot\boldsymbol{Q}\;\;\boldsymbol{\sigma}_3\cdot\boldsymbol{Q}\;\frac{1}{Q^2+m_\pi^2}\;\boldsymbol{\tau}_1\cdot\boldsymbol{\tau}_3 \tag{9}$$

and

$$V_4^{(1)} = -\frac{d_2}{(2\pi)^6}\,\frac{g_A}{4f_\pi^2}\;\boldsymbol{\sigma}_1\times\boldsymbol{\sigma}_3\cdot\boldsymbol{Q}'\;\;\boldsymbol{\sigma}_2\cdot\boldsymbol{Q}'\;\frac{1}{Q'^2+m_\pi^2}\;\boldsymbol{\tau}_1\cdot\boldsymbol{\tau}_2\times\boldsymbol{\tau}_3 - \frac{d_2}{(2\pi)^6}\,\frac{g_A}{4f_\pi^2}\;\boldsymbol{\sigma}_1\times\boldsymbol{\sigma}_2\cdot\boldsymbol{Q}\;\;\boldsymbol{\sigma}_3\cdot\boldsymbol{Q}\;\frac{1}{Q^2+m_\pi^2}\;\boldsymbol{\tau}_1\cdot\boldsymbol{\tau}_3\times\boldsymbol{\tau}_2\,. \tag{10}$$

In a traditional Hamiltonian, of course, there are no zero-range forces. These are an artifact of χPT. A realistic force would contain short-range components from the exchange of heavy mesons. Indeed, one can construct a d_1-term from the exchange of ω or σ mesons, whereas the d_2-term gets contributions from ρ and A_1 exchanges. We can envision a zero-range d_1-term as caused by the exchange of a very heavy isoscalar meson, and the corresponding d_2-term by a very heavy isovector meson. Consequently we extend the zero-range forces to finite range by filling in meson propagators and adding form factors. Eq. (9) is then modified to

$$V_4^{(1)} = \frac{d_1}{(2\pi)^6}\,\frac{g_A}{2f_\pi^2}\;\boldsymbol{\sigma}_1\cdot\boldsymbol{Q}'\;\;\boldsymbol{\sigma}_2\cdot\boldsymbol{Q}'\;\frac{F(Q'^2)}{Q'^2+m_\pi^2}\;\mathcal{O}_{\rm SR}(Q^2)\;\boldsymbol{\tau}_1\cdot\boldsymbol{\tau}_2 + \frac{d_1}{(2\pi)^6}\,\frac{g_A}{2f_\pi^2}\;\mathcal{O}_{\rm SR}(Q'^2)\;\boldsymbol{\sigma}_1\cdot\boldsymbol{Q}\;\;\boldsymbol{\sigma}_3\cdot\boldsymbol{Q}\;\frac{F(Q^2)}{Q^2+m_\pi^2}\;\boldsymbol{\tau}_1\cdot\boldsymbol{\tau}_3, \tag{11}$$

while Eq. (10) becomes

$$V_4^{(1)} = -\frac{d_2}{(2\pi)^6}\,\frac{g_A}{4f_\pi^2}\;\boldsymbol{\sigma}_1\times\boldsymbol{\sigma}_3\cdot\boldsymbol{Q}'\;\;\boldsymbol{\sigma}_2\cdot\boldsymbol{Q}'\;\frac{F(Q'^2)}{Q'^2+m_\pi^2}\;\mathcal{O}_{\rm SR}\,(Q^2)\;\boldsymbol{\tau}_1\cdot\boldsymbol{\tau}_2\times\boldsymbol{\tau}_3 - \frac{d_2}{(2\pi)^6}\,\frac{g_A}{4f_\pi^2}\;\mathcal{O}_{\rm SR}\,(Q'^2)\;\boldsymbol{\sigma}_1\times\boldsymbol{\sigma}_2\cdot\boldsymbol{Q}\;\;\boldsymbol{\sigma}_3\cdot\boldsymbol{Q}\;\frac{F(Q^2)}{Q^2+m_\pi^2}\;\boldsymbol{\tau}_1\cdot\boldsymbol{\tau}_3\times\boldsymbol{\tau}_2, \tag{12}$$

where for our purposes $\mathcal{O}_{\rm SR}(Q^2)$ can be taken to be one of the following choices:

$$\mathcal{O}_{\rm SR}(Q^2) = \frac{m_{sr}^2}{m_{sr}^2+Q^2}, \tag{13}$$

$$\mathcal{O}_{\rm SR}(Q^2) = \frac{m_{sr}^2}{m_{sr}^2+Q^2}\;\left(\frac{\Lambda_{sr}^2}{\Lambda_{sr}^2+Q^2}\right)^2, \tag{14}$$

$$\mathcal{O}_{\rm SR}(Q^2) = \frac{m_{sr}^2}{m_{sr}^2+Q^2}\;\left(\frac{\Lambda_{sr}^2}{\Lambda_{sr}^2+Q^2}\right)^4. \tag{15}$$

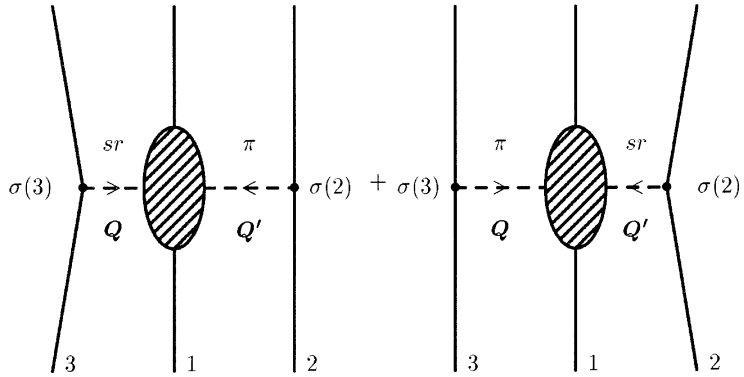

Fig. 5. π-range–short-range 3NF terms

Eq. (13) is simply a heavy-meson propagator that is normalized to 1 at $Q^2 = 0$; in Eq. (14) that propagator is multiplied by the product of two monopole form factors; and in Eq. (15) it is multiplied by the product of two dipole form factors. These terms are depicted in Fig. 5.

The form factors in Eqs. (14) and (15) are chosen in such a way that the resulting 3NF matrix elements at low momenta will not depend strongly on the value of the cut-off parameter Λ_{sr}. In order to stay consistent with the TM′ 2π-exchange 3NF, which we will use, we keep the same form for the πNN form factors used in the TM 3NF,

$$F(Q^2) = \left(\frac{\Lambda^2 - m_\pi^2}{\Lambda^2 + Q^2}\right), \tag{16}$$

which is normalized to 1 at the pion pole ($Q^2 = -m_\pi^2$). Due to the $-m_\pi^2$ factor in the numerator of Eq. (16), the size of a 3NF matrix element containing this form factor depends even for low momenta on the value of the cut-off parameter Λ, just as the TM 3NF does.

Since the d_1- and d_2-terms can be associated with the exchange of many different heavy mesons, we interpret them as effective forces subsuming the effects of all such mesons contributing to the respective term. Thus the exact value for the mass m_{sr} in the propagator is not important; it just has to be roughly the right size. We choose m_{sr} to be the ω-meson mass.

Another quantity that is unknown for the d_1- and d_2-terms is their strength, since χPT cannot predict it. The only thing χPT can say about the strength of these terms is that they should be "natural".

In order to see what naturalness means we rewrite the dimensionful coupling constants d_1 and d_2 in terms of dimensionless ones [9]

$$d_1 = \frac{c_1}{f_\pi^3\,\Lambda}, \tag{17}$$

$$d_2 = \frac{c_2}{f_\pi^3\,\Lambda}, \tag{18}$$

where $\Lambda = 1$ GeV, $f_\pi = 92.4$ MeV, and c_1 and c_2 are dimensionless. For c_1 and c_2 to be natural means that their value should be on the order of 1. In practical terms

the absolute values of c_1 or c_2 should typically (and roughly) be numbers comparable to 1, 2, ... (or the inverse); their signs, however, are not known.

So in order to use the d_1- and d_2-terms predicted by a χPT-based (i.e., the Texas) force, we have to make adaptations such as those described above. In order to differentiate between that zero-range force and the finite-range terms written down in Eqs. (11) and (12), we refer to the latter as the Texas-Los Alamos force.

At this point we should mention that the d_1- and d_2-terms are predicted not only by χPT, but by conventional nuclear field-theory models as well. For example, the d_1-term is contained in ref. [19] as π and σ exchanges or π and ω exchanges with an intermediate $N(1440)$ resonance (Eqs. (3.2a) and (3.2b) in ref. [19]), while the d_2-term is included in ref. [16] as a π-ρ Kroll-Ruderman term (Eq. (2.13f) together with the last term, the "4", of Eq. (2.15a) in ref. [16]).

The d_2-term is also included in the meson-theoretical RuhrPot π-ρ 3NF [10] as Eq. (A7), among many other terms. Here the mechanism for the d_2-term is a $NN\pi\rho$ vertex at one of the three nucleons.

However, these papers include many other 3NF terms, as well, that are of higher order in power counting (i.e., they are smaller) than the d_1 and d_2 terms. Ref. [16] includes 126 terms, for example, and the d_2-term is part of one of them. After having written down these terms the authors conclude that the d_2-part is the dominant one. This exhibits the advantage of a power-counting scheme like the one that is part of χPT: One knows from the very beginning which terms should be important and which should not. With conventional nuclear field-theory models there is no easy way to know this beforehand.

The d_1- and d_2-terms are therefore not new in the sense that they have never been written down before. But they are new in the sense that for the first time they have been identified as the leading-order terms of the pion-range–short-range 3NF and can be used (see below) in a realistic calculation of the $3N$ continuum.

5 Calculating the Three-Nucleon Continuum

It became possible for the first time in ref. [20] to include a realistic 3NF in a rigorous calculation of the $3N$ continuum for energies above the deuteron breakup threshold. The algorithm used in ref. [20] was later replaced by the more effective one developed in ref. [21].

The Faddeev equation with a 3NF included reads

$$\begin{aligned} T = {} & tP\phi + (1 + tG_0)V_4^{(1)}(1 + P)\phi \\ & + tPG_0T + (1 + tG_0)V_4^{(1)}(1 + P)G_0T, \end{aligned} \tag{19}$$

where T is the Faddeev amplitude for which Eq. (19) has to be solved, t is the two-body t-matrix, G_0 is the free three-nucleon propagator, P is the sum of a cyclic and an anti-cyclic permutation (operator) for the three nucleons [22], $V_4^{(1)}$ has already been defined in Sect. 2, and ϕ is the incoming state composed of a free nucleon and a free deuteron. Once Eq. (19) is solved one gets the elastic transition amplitude via

$$U = PG_0^{-1} + PT + V_4^{(1)}(1 + P)\phi + V_4^{(1)}(1 + P)G_0T \tag{20}$$

and the transition amplitude for the breakup process via

$$U_0 = (1 + P)T. \tag{21}$$

The 3NF is built into Eq. (19) in a perturbative way. Solving Eq. (19) by iteration not only gives the different orders in T, but the different orders in $V_4^{(1)}$ as well. This will become important later on. Of course we always iterate Eq. (19) until we reach full convergence.

In addition to using the new algorithm for the Faddeev equations, we have also replaced the PWD for the 3NF used in ref. [20] by one developed later in ref. [23]. The reason is that the original PWD is numerically unstable for higher partial waves than those required in the early work. The PWD for the d_1- and d_2-terms is performed in Appendix A. For details on the numerics see ref. [3].

6 Results

The first thing one realizes when dealing with the d_1- and d_2-terms is that these terms appear to be big. By big we mean that one cannot get convergence for the iteration of Eq. (19) when c_1 and c_2 are significantly larger than 1 and 0.5, respectively. Indeed, the convergence criterion (Eq. (5.15) of ref. [24] – the difference between the last and before-last result of the iteration of Eq. (19), averaged in a specific way, has to become less than an ϵ) cannot usually be fulfilled for $\epsilon = 10^{-4}$ (our usual value for ϵ), but only for $\epsilon = 10^{-3}$ or larger.

This slower (or lack of) convergence can easily be related to the size of these 3NF terms. For example, if one slowly increases the value of c_1 from below 1 or c_2 from below 0.5, one can examine how the convergence becomes worse around (or above) 1 or 0.5, respectively.

One finds that the smallest ϵ for which the convergence criterion can be fulfilled increases with increasing c_1 and c_2. If one increases the values for c_1 and c_2 further one finally reaches the point where convergence is totally lost.

The above-described loss of convergence happens first for $J^\Pi = \frac{1}{2}^+$, whose convergence is always slowest due to the presence of the bound state. However, even for larger values of c_1 and c_2 where there is no longer convergence in the $\frac{1}{2}^+$ channels, the 3NF contribution to the Faddeev amplitude T is still significantly smaller than the *NN*-force contribution. Thus naively one would expect no difficulty with the convergence. However, iterating Eq. (19) mixes the perturbation series for the 3NF with the iteration series for the solution of T and therefore we lose convergence even for relatively small 3NFs.

It might be that this behaviour is an artifact of our way of parameterizing the new 3NF terms (e.g., of our choice for the form factors). Unfortunately, we did not have the resources necessary to study this. Since we intend to study only the cardinal effects of these new 3NF terms, this problem is not particularly important. We simply confine ourselves to smaller values for c_1 and c_2 for which we can present fully converged results.

Even if the convergence problem turns out not to arise from our choice of parameterization, it is still not a problem of principle. We would just have to use a different algorithm for the incorporation of a 3NF into the Faddeev equations,

either the one we used in the past [20] or, due to the advance of super-computers, just treat the 3NF in a straight-forward way (i.e., solve the Lippmann-Schwinger equation driven by $V_4^{(1)}$ and then use the corresponding t-matrix in the Faddeev equations).

All calculations presented in the following have been performed with a somewhat reduced accuracy. That means that the maximally allowed angular momentum for the two-body subsystem has been reduced to $j_{\max} = 2$ everywhere except for the inner states during the calculation of the 3NF matrix elements (see ref. [23] for details), which have been reduced to $j_{\max} = 3$. With these restrictions we are still within 2–3% of the results for a fully converged calculation at 3 and 10 MeV and not much worse at 50 MeV. This is sufficient for our purpose.

In the following we concentrate on the neutron analyzing power A_y. Of course, if we want to find a solution for the A_y-puzzle we also need to look at the deuteron analyzing power iT_{11}. We do not do this here for several reasons. First, we do not intend to present a solution, but rather to see if a solution is possible. Second, there are no *nd* data for iT_{11}, but only *pd* data. Since we cannot include the Coulomb force in our calculations it makes more sense to concentrate on A_y here. Third, the effects on iT_{11} are always very similar to the effects on A_y; there are no significant differences. This suggests that if we are able to describe A_y we probably will also describe iT_{11}.

In Figs. 6–8 we show the nucleon analyzing power A_y for elastic neutron-deuteron scattering. The negative sign for c_1 was chosen in order to get an enhancement in the maximum of A_y instead of a decrease. Although the

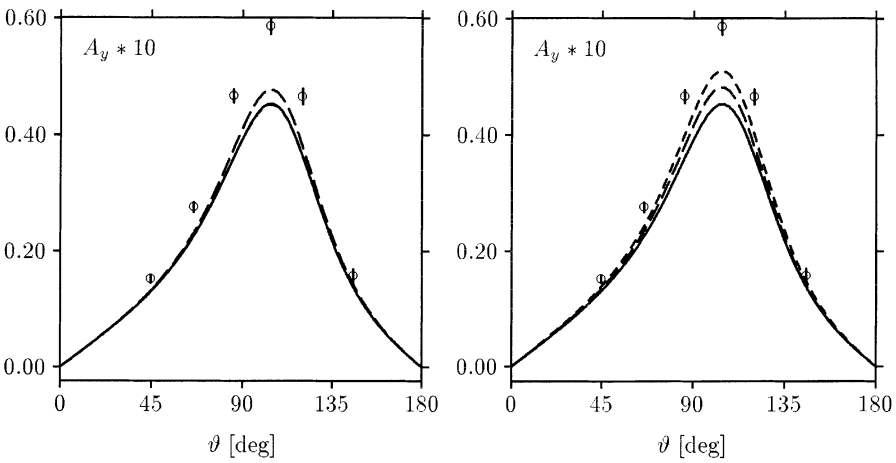

Fig. 6. The elastic neutron analyzing power A_y at $E_{\text{lab}} = 3\,\text{MeV}$. The solid line in both figures represents the prediction for the *NN* potential (AV18) alone. In the left-hand figure the long-dashed line is the prediction for AV18 plus the d_1-term 3NF with $c_1 = -1$. The short-dashed line is the prediction of AV18 plus the d_2-term 3NF with $c_2 = 0.5$. (Note that the short-dashed line overlaps almost completely with the solid line, and is nearly invisible.) In the right-hand figure the long dashed line is the prediction of AV18 plus the TM′ 3NF with the cut-off parameter $\Lambda = 5.215\,m_\pi$. For the short-dashed line on top of TM′ the d_1- and d_2-terms have been added with parameters $c_1 = -1$ and $c_2 = 0.5$, respectively. Form factors and other parameters have been chosen as described in Sect. 4. The circles are *nd* data from ref. [25]

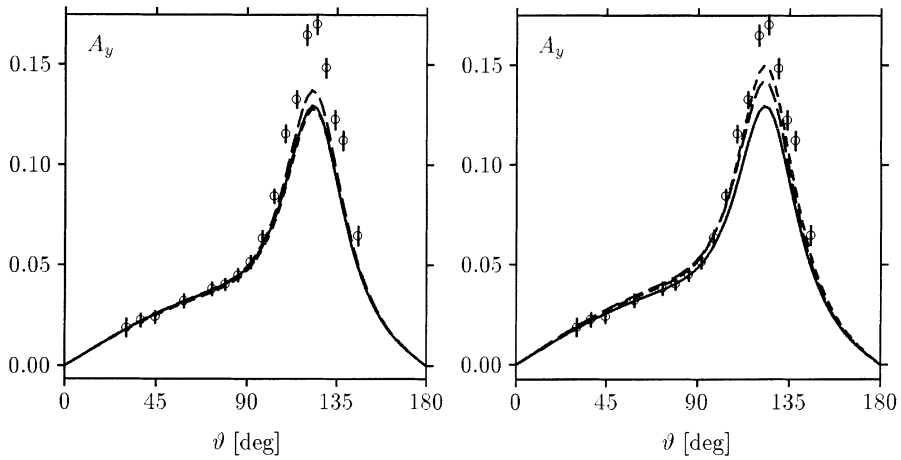

Fig. 7. Same as Fig. 6 but for $E_{\rm lab} = 10\,$MeV. The circles are *nd* data from ref. [26]

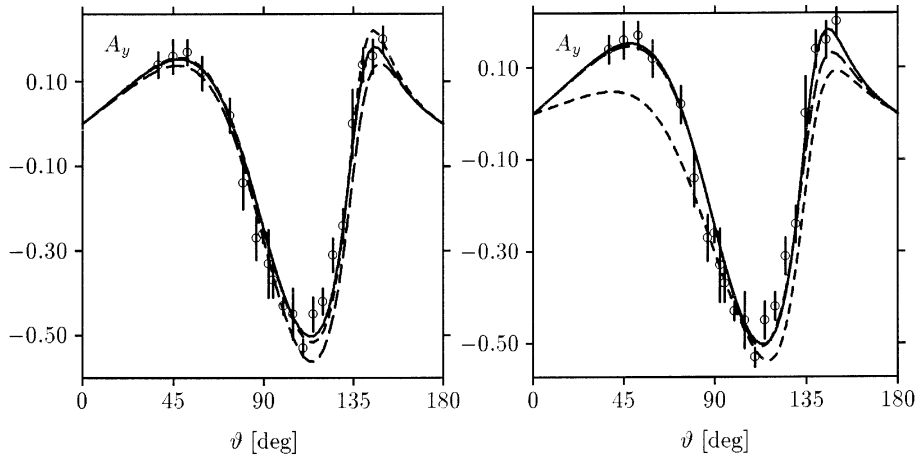

Fig. 8. Same as Fig. 6 but for $E_{\rm lab} = 50\,$MeV. The circles are *nd* data from ref. [27]

enhancement by d_1 of the maximum of A_y at 3 MeV (depicted in Fig. 6) is not terribly large and A_y calculated with the d_1-term is still far from the data, this is nevertheless a very promising result, since one can easily reach the experimental points with a larger value for c_1 (i.e., more negative than -1) that is still natural. We will return to this point.

As can be seen from Fig. 6 the d_2-term has practically no effect on A_y at 3 MeV. This is ideal since one can fix the value of c_1 at 3 MeV without worrying about effects from d_2.

One should note that the 2π-exchange 3NF (TM′) already causes a visible increase in the maximum of A_y. However, plausible choices for the parameters in the 2π-exchange 3NF will not be able to explain the A_y-puzzle, since these parameters are much more restricted than they are for the new 3NF terms. Our choice for the cut-off parameter of the πNN form factors in the TM′ 3NF ($\Lambda = 5.215\,m_\pi$) probably makes our 2π-exchange 3NF somewhat too small. But even with the recommended choice of the Tucson-Melbourne group, one can only

expect that the effect of the 2π-exchange 3NF would be larger by about 20%. This means that with a 2π-exchange 3NF one can come nowhere close to the experimental values.

At 10 MeV the situation is similar to 3 MeV. One can see, however, that the d_2-term has a small effect on A_y at this higher energy.

At 50 MeV the situation has totally changed. Firstly, there is no A_y-puzzle at this energy (the predictions of all modern *NN* forces agree reasonably well with the data). However, it should be emphasized that the experimental situation is not as clear as at the lower energies, since the error bars are significantly larger. This means that there is still some room for small 3NF effects at this energy.

Secondly, the form of A_y has changed. The maximum that we have seen at the two lower energies has become a minimum here, and there are two less-pronounced maxima, one at each side of the minimum. This is due to the fact that at this energy the mechanisms that build up the analyzing power have changed. We know from ref. [3] that at 50 MeV the *P*-waves have become less important and that *D*-waves play a role.

If we now examine Fig. 8 we see that both the d_1- and the d_2-terms have large effects on A_y at this energy. This does not come as a surprise. We know that a 3NF always is of shorter range than the one-pion-exchange part of the *NN* force. Therefore one naively expects that 3NFs become more and more important with increasing energy. That this is indeed true for the 2π-exchange 3NF has been shown in ref. [3] and more recently in refs. [1] and [2] for the total and differential elastic cross sections, respectively. Since the new 3NF terms d_1 and d_2 are of even shorter range than the 2π-exchange 3NF, one expects that their effects grow even faster with increasing energy. Our calculations suggest that this is true.

Of course, in this case we will face serious problems in our attempt to find a solution for the A_y-puzzle via 3NFs of shorter range than the 2π-exchange 3NF. We will discuss this below.

There is one other interesting aspect of Fig. 8. If we look at the left maximum in the left-hand figure of Fig. 8 we see that the effects both of the d_1- and d_2-terms in that maximum are moderate. However, if we add these two terms on top of the 2π-exchange 3NF this combined 3NF has very large effects on that maximum, as can be seen in the right-hand figure of Fig. 8, whereas the effect of the 2π-exchange 3NF alone is almost zero. This means that in this special case a very strong constructive interference develops between the various 3NF terms. It tells us that in dealing with 3NFs one has to be very careful if one excludes certain 3NF terms, since even if their individual effects are small, their interference with other 3NF terms might lead to surprisingly large effects.

Next we want to quantify our findings. For this purpose we list in Table 2 the effects of the various 3NFs alone and together in the extrema of A_y. This table includes more calculations than we have shown in the figures. We included one calculation with $c_1 = -2$ at 3 MeV. For this calculation we could only reach a convergence with $\epsilon = 10^{-3}$. Therefore we did not repeat this calculation for the higher energies.

The first thing we see in Table 2 is that the effect of the elimination of the short-range part of the c-term in the original TM 3NF is negligible at 3 MeV, but already significant at 10 MeV. This means that older calculations with the original

Table 2. Theoretical predictions for A_y at the extrema for various energies. The c.m. angles of the extrema are given in brackets in the second header line of the table. For calculations where a 3NF is added to AV18, the deviation of that result from the calculation with AV18 alone is given in percent in brackets as well. All calculations were performed with $j_{\max} = 2$ except the ones in the two lines marked with *, which were performed with $j_{\max} = 3$. For simplicity we denoted different values for the dimensionless constants c_1 and c_2 as multiplicative factors in front of d_1 and d_2 in the first column of the table (e.g., $-2d_1$ means $c_1 = -2$)

	3 MeV $A_y\|_{\max}(105^\circ)$	10 MeV $A_y\|_{\max}(122.5^\circ)$	50 MeV $A_y\|_{\max}(47.5^\circ)$	50 MeV $A_y\|_{\min}(112.5^\circ)$
AV18*	0.04549	0.1275	0.1599	−0.5066
AV18	0.04536	0.1294	0.1539	−0.5016
+TM*	0.04857 (+6.8%)	0.1328 (+4.2%)	0.1543 (−3.6%)	−0.4953 (−2.3%)
+TM′	0.04825 (+6.4%)	0.1420 (+9.7%)	0.1472 (−4.5%)	−0.5066 (+1.0%)
$+d_1$	0.04343 (−4.4%)	0.1231 (−5.1%)	0.1589 (+3.2%)	−0.4306 (−16.5%)
$-d_1$	0.04778 (+5.3%)	0.1370 (+5.9%)	0.1388 (−10.9%)	−0.5606 (+11.8%)
$-2d_1$	0.05094 (+12.3%)			
$+0.5d_2$	0.04521 (−0.3%)	0.1277 (−1.3%)	0.1578 (+2.5%)	−0.5157 (+2.8%)
$-0.5d_2$	0.04561 (+0.6%)	0.1469 (+13.5%)	0.1503 (−2.4%)	−0.4832 (−3.8%)
TM′ $-d_1$ $+0.5d_2$	0.05106 (+12.6%)	0.1497 (+15.5%)	0.04804	−0.5367 (+7.0%)

TM 3NF should be repeated using TM′ for energies above the deuteron breakup threshold.

Next we see that the effect of the d_1-term at 3 and 10 MeV is more or less linear with the value of c_1, but not so at 50 MeV. On the other hand the effect of the d_2-term is not linear with the value of c_2 at 3 MeV and is dramatically less so at 10 MeV, but becomes more or less linear at 50 MeV.

A look at the last line of Table 2 reveals that at all energies there are some interference effects between the various 3NF terms, though they are strongest in the maximum at 50 MeV. Interestingly, we have a significant destructive interference in the minimum of A_y at 50 MeV.

Next we want to see if it is possible to find a combination of d_1 and d_2 with which it is possible to come close to the experimental data for A_y. Of course, due to the nature of our calculations, any such combination that we might find can only give a rough estimate for the values of c_1 and c_2, but that is all we want. If we can find such a combination we would have shown that a solution of the A_y-puzzle using these two 3NF terms of pion-range–short-range nature is possible.

So let us start with 3 MeV. Here the situation is relatively simple, since we can neglect the effect of the d_2-term on A_y. Taking into account that we probably underestimate the effect of the 2π-exchange 3NF somewhat (as we stated above), we can extrapolate from Table 2 that a value for c_1 of about -3 would probably be able to close the gap ($\sim 30\%$) between the data and the predictions of the *NN* potentials.

If we move on to 10 MeV we see that (not taking into account d_2 for the moment) a combination of TM′ $-3d_1$ (this notation means that we are using TM′ and a d_1 force with $c_1 = -3$) would probably overestimate the data a little bit,

since the gap is also about 30% at this energy, but the 2π-exchange 3NF has a somewhat larger effect at 10 MeV than at 3 MeV, whereas the effect of d_1 is more or less the same at both energies. However, at 10 MeV the d_2-term has a small but visible effect on A_y. So we can use the d_2-term to counterbalance the increased effect of the 2π-exchange 3NF. This leads us to a value for c_2 that should be positive and small, perhaps 0.5 or 1. Thus a combination like $\mathrm{TM}' - 3d_1 + 0.5d_2$ or $\mathrm{TM}' - 3d_1 + d_2$ would be able to bring the theoretical prediction for A_y close to the experimental data at 3 and 10 MeV.

It might be, however, that the values we just gave for c_1 and c_2 are even smaller in reality. The reason is that, as mentioned above, we used the πNN form factor Eq. (16) for the d_1- and d_2-terms with the same small value for Λ as for the 2π-exchange part of the 3NF. This might cause us to underestimate the strength of d_1 and d_2 somewhat.

Now let us look at 50 MeV. We see immediately from Table 2 that the combination of 3NF terms mentioned above does not work at this energy. The effects would be far too large. If that is so, is there any way out of this dilemma?

One might argue that 3NF terms of even shorter range than d_1 and d_2 might become important at this higher energy. If that is the case these additional 3NF terms will provide additional parameters with which one might be able to describe the data at 50 MeV. As we mentioned in Sect. 4 such terms exist: the so-called e_1-, e_2-, and e_3-terms, which are of short-range–short-range nature. However, we believe that the inclusion of these terms will lead to serious problems for two (connected) reasons.

We face the conceptual and practical problem that the short-range e_1-, e_2-, and e_3-terms are indistinguishable from very short-range (i.e., δ-function) parts of the 2π-exchange 3NF. Disentangling these terms is usually made more serious by the lack of consistency between the *NN*-force and the 3NF models we use. In addition, accumulating too many parameters (the values of e_1, e_2, and e_3 are unknown) in a three-nucleon problem is self-defeating.

This leads us immediately to a deeper, basic question: How high in energy do models for the nuclear force based on meson exchange make sense? Meson-exchange models have been extremely successful, even at much higher energies than we are considering here. Could it be that the meson-exchange picture – or rather the way we usually implement it – breaks down (i.e., becomes excessively complicated) at an energy as low as 50 MeV as soon as one starts to look into (admittedly small) details of the nuclear force? To answer this question one would have to investigate whether the short-range–short-range 3NF terms play any role in A_y (and other observables) at 50 MeV. Since this is such a basic question it might be worthwhile to do so.

However, there is one other possibility. We have not yet mentioned the so-called 3NF Born terms [28, 11]. These terms are also predicted by χPT to be the same order in power counting as all the other 3NF terms mentioned here. These terms are model-dependent in the sense that they depend on how the ''off-shellness'' of the *NN* potential has been defined, and they thus depend on the details of the *NN* potential that one uses [28, 11]. Usually these Born terms are neglected, on the one hand due to the complications they bring (such as nonlocality), and on the other hand because a subset of them is known to be small [6]. One of the 16 Born terms

is of spin-orbit nature [28], however. This particular Born term might be important for A_y, since that observable is very sensitive to the spin-orbit force [4]. The next step in exploring the A_y-puzzle should be to take into account (at least) this particular Born term.

We have found that the effects of the d_1- and d_2-terms on other observables in elastic *nd* scattering are usually smaller than their effects on A_y and iT_{11}. Only for some tensor-polarization observables are the effects comparable to those on A_y and iT_{11}.

7 Summary and Conclusions

In Sect. 2 we have reviewed the current state of affairs for the 2π-exchange 3NF. Due to the elimination of the pion-range–short-range part of the c-term of the TM 3NF, the question of the operator form of the 2π-exchange 3NF is now settled. We showed that in low-energy elastic *nd* scattering the effect of the 2π-exchange 3NF is dominated by the b-term, as in the bound state. In addition we found that those observables that scale with the triton binding energy show 3NF effects only for the channels for which the $3N$ system is bound (viz., those with $J^\Pi = \frac{1}{2}^+$).

Next we commented in Sect. 3 on the results found so far using 3NFs that include the exchange of one or more mesons that are heavier than the pion. Due to the nature of these effects we suspect that the π-ρ TM 3NF is also dominated by its b-term and therefore cannot explain the A_y-puzzle.

In Sect. 4 we introduced the Texas force, which is based on χPT. We explained which of the 3NF terms of the Texas force are of interest to us, and we extended the zero-range parts of these terms to finite range in order to connect with the traditional models we use for the *NN* force and the 2π-exchange 3NF. Thereafter we gave a meson-exchange interpretation to the new terms. Finally we commented on the appearance of those terms in calculations that are not based on χPT.

A brief review of our approach to solving the Faddeev equations for the $3N$ continuum has been given in Sect. 5. For the PWD of the new 3NF terms we refer to Appendix A.

Finally we presented our results in Sect. 6. We studied the effects of the new 3NF terms on A_y at 3, 10, and 50 MeV. For the two lower energies we could find a combination of the d_1- and d_2-terms that (together with the *NN* force and the 2π-exchange 3NF) would be able to describe the A_y data. Although this is only a qualitative finding, it is of considerable importance because we have developed for the first time a microscopic model of the nuclear force that has the potential to describe the low-energy vector-analyzing-power data. To make this model quantitative will involve considerable effort. We typically obtain the b and d parameters from fits to π-N scattering, and in principle the d_1 and d_2 parameters can be obtained from pion production in *NN* scattering, although the latter remains to be seen. If that proves impractical we would have to fit d_1 and d_2 (and the cut-off parameter Λ in the πNN form factor) to the triton binding energy, to A_y, and to other *nd* observables for which we have *nd* data. Given the complexity of three-nucleon calculations, this three-parameter search would be very time-consuming.

However, as discussed in Sect. 6, such a 3NF would not be able to describe the A_y data (and possibly data for other observables) at 50 MeV and higher. This might

be due to the fact that other 3NF terms than those included in this paper become important at that energy. One such 3NF term could be one of the Born terms that is of spin-orbit type, and therefore is a candidate to be of importance for A_y. Up to now the Born terms have been largely neglected, but it seems obvious that at least the one just mentioned has to be included in $3N$ continuum calculations as a next step towards a solution of the A_y-puzzle.

Other candidates for 3NF terms that might become important at 50 MeV are the ones of short-range–short-range type, which are predicted by χPT to be the same order as the d_1- and d_2-terms and the 2π-exchange 3NF terms that have been included in this study. If it turns out that these terms do become important at 50 MeV we face serious problems with meson-exchange models.

Unfortunately, another problem would also arise: We would have to fit many more terms, which on the one hand is very difficult for a $3N$ problem, and on the other hand we might loose any predictive power by accumulating too many parameters with increasing energy. Since these are important questions, it might be worthwhile to check first whether or not the short-range–short-range 3NF terms predicted by χPT in lowest non-vanishing order have any effect at 50 MeV.

In this paper we believe that we have made an important step forward toward the solution of the long-standing A_y-puzzle by identifying new 3NF terms that have a significant effect on A_y even at low energies. We found these terms using a systematic approach for the classification of the 3NF terms (i.e., the power-counting scheme of χPT). In doing so new questions arose that require further testing of our models of nuclear forces. However, we have to leave the answers to these questions to future work.

Acknowledgement. The work of D.H. and J.L.F. was performed under the auspices of the U.S. Department of Energy. The work of D.H. was supported in part by the Deutsche Forschungsgemeinschaft under Project No. Hu 746/1-3. The work of A.N. was supported by the Deutsche Forschungsgemeinschaft under Project No. Gl 87/27-1. The work of U.v.K. was supported in part under NSF grant PHY 94-20470. The numerical calculations have been performed on the Cray T90 and Cray T3E of the Höchstleistungsrechenzentrum in Jülich, Germany.

Appendix A. Partial-Wave Decomposition

For the partial-wave decomposition (PWD) of the new 3NF terms we will closely follow ref. [23]. We will not repeat here the principles and ideas behind the PWD as developed in ref. [23] but rather apply them to the new d_1 and d_2 terms. We will often refer to equations from ref. [23] in the form (xx [23]), where xx is the equation number in ref. [23]. In addition, we refer to ref. [23] for the notation used here.

A.1 The d_1-Term

Let us begin with the d_1-term. It is given in Eq. (11) as

$$V_4^{(1)} = \frac{d_1}{(2\pi)^6}\,\frac{g_A}{2f_\pi^2}\;\boldsymbol{\sigma}_1\cdot\boldsymbol{Q}'\;\;\boldsymbol{\sigma}_2\cdot\boldsymbol{Q}'\;\frac{F(Q'^2)}{Q'^2+m_\pi^2}\;\mathcal{O}_{\rm SR}(Q^2)\;\boldsymbol{\tau}_1\cdot\boldsymbol{\tau}_2$$
$$+\frac{d_1}{(2\pi)^6}\,\frac{g_A}{2f_\pi^2}\;\mathcal{O}_{\rm SR}(Q'^2)\;\;\boldsymbol{\sigma}_1\cdot\boldsymbol{Q}\;\;\boldsymbol{\sigma}_3\cdot\boldsymbol{Q}\;\frac{F(Q^2)}{Q^2+m_\pi^2}\;\boldsymbol{\tau}_1\cdot\boldsymbol{\tau}_3. \qquad \text{(A.1)}$$

For the notation see Fig. 5. As in ref. [23] we will deal with the momentum-spin matrix elements and the isospin matrix elements separately (see Eq. (35[23])).

We start with the momentum-spin matrix elements. In analogy to Eqs. (28[23]), (31[23]), and (35[23]) we split the momentum-spin-dependent part of the d_1-term into two quasi-two-body operators. This leads to matrix elements

$$\begin{aligned} M_{d_1}^{J,2} &= {}_2\langle pq\alpha_J|\boldsymbol{\sigma}_1\cdot\boldsymbol{Q}\ \ \boldsymbol{\sigma}_3\cdot\boldsymbol{Q}\ \frac{F(Q^2)}{Q^2+m_\pi^2}|p_1q_1\alpha_{1J}\rangle_2 \\ &= \frac{\delta(q-q_1)}{q^2}\ \delta_{\lambda\lambda_1}\ \delta_{II_1}\ \sum_{mm_1} C(jm\ \ IM-m,JM)\ C(j_1m_1\ I_1M_1-m_1,J_1M_1) \\ &\quad\times \underbrace{{}_2\langle pjm|\boldsymbol{\sigma}_1\cdot\boldsymbol{Q}\ \ \boldsymbol{\sigma}_3\cdot\boldsymbol{Q}\ \frac{F(Q^2)}{Q^2+m_\pi^2}|p_1j_1m_1\rangle_2}_{\equiv M_{d_1}^{j,2}}\ , \end{aligned} \tag{A.2}$$

$$\begin{aligned} \tilde{M}_{d_1}^{J,3} &= {}_3\langle p_2q_2\alpha_{2J}|\mathscr{O}(Q'^2)\big|p'q'\alpha'_J\big\rangle_3 \\ &= \frac{\delta(q_2-q')}{q'^2}\ \delta_{\lambda'\lambda_2}\ \delta_{I'I_2}\ \sum_{m_2m'} C(j_2m_2\ \ I_2M_2-m_2,J_2M_2)\ C(j'm'\ \ I'M'-m',J'M') \\ &\quad\times \underbrace{{}_3\langle p_2j_2\,m_2|\mathscr{O}(Q'^2)|p'j'm'\rangle_3}_{\equiv \tilde{M}_{d_2}^{j,3}} \end{aligned} \tag{A.3}$$

for the second term in Eq. (A.1). The momentum transfers $\boldsymbol{Q}$ and $\boldsymbol{Q}'$ are given by

$$\boldsymbol{Q} = \boldsymbol{p}-\boldsymbol{p}_1, \tag{A.4}$$

$$\boldsymbol{Q}' = \boldsymbol{p}'-\boldsymbol{p}_2. \tag{A.5}$$

For $M_{d_1}^{j,2}$ we have to decompose the operator

$$\begin{aligned} \boldsymbol{\sigma}_1\cdot\boldsymbol{Q}\ \ \boldsymbol{\sigma}_3\cdot\boldsymbol{Q} &= 4\pi\ |\boldsymbol{p}-\boldsymbol{p}_1|^2\ \Big\{\{\sigma_1,Y_1(\widehat{\boldsymbol{p}-\boldsymbol{p}_1})\}^0,\{\sigma_1,Y_1(\widehat{\boldsymbol{p}-\boldsymbol{p}_1})\}^0\Big\}^0 \\ &= \sqrt{4\pi}\ |\boldsymbol{p}-\boldsymbol{p}_1|^2\ \sum_i C(10\ \ 10,i0) \\ &\quad\times\sum_{a+b=i}\frac{p^a(-p_1)^b}{|\boldsymbol{p}-\boldsymbol{p}_1|^i}\ \sqrt{\frac{4\pi\hat{i}!}{\hat{a}!\ \hat{b}!}}\ \big\{\{\sigma_1,\sigma_3\}^i,\ \mathscr{Y}^i_{ab}(\hat{p},\hat{p}_1)\big\}^0 \\ &= 4\pi\left[-\frac{1}{\sqrt{3}}\ |\boldsymbol{p}-\boldsymbol{p}_1|^2\ \Big\{\{\sigma_1,\sigma_3\}^0,\mathscr{Y}^0_{00}(\hat{p},\hat{p}_1)\Big\}^0\right. \\ &\quad\left.+\ 4\sqrt{5}\ \sum_{a+b=2}\frac{p^a(-p_1)^b}{\sqrt{\hat{a}!\ \hat{b}!}}\ \Big\{\{\sigma_1,\sigma_3\}^2,\mathscr{Y}^2_{ab}(\hat{p},\hat{p}_1)\Big\}^0\right]. \end{aligned} \tag{A.6}$$

For the expansion of the angular dependence in the propagator and form factor we use Eqs. (43–47[23]) and (59[23]). Putting this together with the result (A.6) we get

$$\begin{aligned} M_{d_1}^{j,2} = \frac{(4\pi)^2}{2}\ &\Bigg[\sum_{\bar{l}}(-)^{\bar{l}}\sqrt{\hat{\bar{l}}}\ \tilde{H}_{\bar{l}}(pp_1)\ {}_2\langle pjm|\ \Big\{\{\sigma_1,\sigma_3\}^0,\ \mathscr{Y}^0_{00}(\hat{p},\hat{p}_1)\Big\}^0 \\ &\times\mathscr{Y}^{00}_{\bar{l}\bar{l}}(\hat{p},\hat{p}_1)|\,p_1j_1m_1\rangle_2+\sqrt{\frac{2}{3}}\ \sqrt{5!}\ \sum_{a+b=2}\frac{p^a(-p_1)^b}{\sqrt{\hat{a}!\ \hat{b}!}}\ \sum_{\bar{l}}(-)^{\bar{l}}\sqrt{\hat{\bar{l}}}\ H_{\bar{l}}(pp_1) \\ &\times{}_2\langle pjm|\ \Big\{\{\sigma_1,\sigma_3\}^2,\ \mathscr{Y}^2_{ab}(\hat{p},\hat{p}_1)\Big\}^0\ \mathscr{Y}^{00}_{\bar{l}\bar{l}}(\hat{p},\hat{p}_1)|\,p_1j_1m_1\rangle_2\Bigg]. \end{aligned} \tag{A.7}$$

Next we need to recouple the spherical harmonics that appear in the two matrix elements of Eq. (A.7):

$$\Big\{\{\sigma_1,\sigma_3\}^0,\, \mathscr{Y}^0_{00}(\hat{p},\hat{p}_1)\Big\}^0 \mathscr{Y}^{00}_{\bar{l}\bar{l}}(\hat{p},\hat{p}_1) = \frac{1}{4\pi}\,\{\sigma_1,\sigma_3\}^0\,\mathscr{Y}^{00}_{\bar{l}\bar{l}}(\hat{p},\hat{p}_1), \tag{A.8}$$

$$\begin{aligned}\Big\{\{\sigma_1,\sigma_3\}^2,\, \mathscr{Y}^2_{ab}(\hat{p},\hat{p}_1)\Big\}^0 \mathscr{Y}^{00}_{\bar{l}\bar{l}}(\hat{p},\hat{p}_1) = \frac{1}{4\pi}\sum_{i_1 i_2}(-)^{\bar{l}+a+i_2}\sqrt{\hat{a}\hat{b}\hat{\bar{l}}}\begin{Bmatrix} i_1 & i_2 & 2\\ b & a & \bar{l}\end{Bmatrix}\\ \times C(a0\;\bar{l}0, i_1 0)C(b0\;\bar{l}0, i_2 0)\\ \times\Big\{\{\sigma_1,\sigma_3\}^2,\, \mathscr{Y}^2_{i_1 i_2}(\hat{p},\hat{p}_1)\Big\}^0\end{aligned} \tag{A.9}$$

and therefore $M^{j;2}_{d_1}$ becomes

$$\begin{aligned}M^{j;2}_{d_1} = &-\frac{4\pi}{2}\,\frac{1}{\sqrt{3}}\sum_{\bar{l}}(-)^{\bar{l}}\sqrt{\hat{\bar{l}}}\,\tilde{H}_{\bar{l}}(pp_1)\;{}_2\langle pjm|\{\sigma_1,\sigma_3\}^0\,\mathscr{Y}^{00}_{\bar{l}\bar{l}}(\hat{p},\hat{p}_1)|p_1 j_1 m_1\rangle_2\\ &+8\pi\,\sqrt{5}\sum_{\bar{l}}(-)^{\bar{l}}\sqrt{\hat{\bar{l}}}\,H_{\bar{l}}(pp_1)\sum_{a+b=2}\frac{p^a(-p_1)^b}{\sqrt{\hat{a}!\;\hat{b}!}}\sum_{i_1 i_2}(-)^{\bar{l}+a+i_2}\\ &\times\sqrt{\hat{a}\hat{b}\hat{\bar{l}}}\begin{Bmatrix} i_1 & i_2 & 2\\ b & a & \bar{l}\end{Bmatrix}C(a0\;\bar{l}0, i_1 0)\,C(b0\;\bar{l}0, i_2 0)\\ &\times{}_2\langle pjm|\Big\{\{\sigma_1,\sigma_3\}^2,\, \mathscr{Y}^2_{i_1 i_2}(\hat{p},\hat{p}_1)\Big\}^0|p_1 j_1 m_1\rangle_2.\end{aligned} \tag{A.10}$$

Now we have to evaluate the two matrix elements in Eq. (A.10):

$$\begin{aligned}&{}_2\langle pjm|\{\sigma_1,\sigma_3\}^0\,\mathscr{Y}^{00}_{\bar{l}\bar{l}}(\hat{p},\hat{p}_1)|p_1 j_1 m_1\rangle_2\\ &\quad=\delta_{jj_1}\,\delta_{mm_1}\,\delta_{ll_1}\,\delta_{ss_1}\,\delta_{\bar{l}\bar{l}}\,2\sqrt{3}\,(-)^{l+s}\,\frac{1}{\sqrt{\hat{l}}}\begin{Bmatrix}\frac{1}{2} & \frac{1}{2} & s\\ \frac{1}{2} & \frac{1}{2} & 1\end{Bmatrix},\end{aligned} \tag{A.11}$$

$$\begin{aligned}&{}_2\langle pjm|\Big\{\{\sigma_1,\sigma_3\}^2,\, \mathscr{Y}^2_{i_1 i_2}(\hat{p},\hat{p}_1)\Big\}^0|p_1 j_1 m_1\rangle_2\\ &\quad=\delta_{jj_1}\,\delta_{mm_1}\,\delta_{li_1}\,\delta_{l_1 i_2}\,6\sqrt{5}\,(-)^{j+s_1}\sqrt{\hat{s}\hat{s}_1}\begin{Bmatrix} l_1 & s_1 & j\\ s & l & 2\end{Bmatrix}\begin{Bmatrix} 1 & 1 & 2\\ \frac{1}{2} & \frac{1}{2} & s\\ \frac{1}{2} & \frac{1}{2} & s_1\end{Bmatrix}.\end{aligned} \tag{A.12}$$

Inserting these results into Eq. (A.10) yields

$$\begin{aligned}M^{j;2}_{d_1} = &\;\delta_{jj_1}\,\delta_{mm_1}\,\delta_{ll_1}\,\delta_{ss_1}\,4\pi\,(-)^{s+1}\,\tilde{H}_l(pp_1)\begin{Bmatrix}\frac{1}{2} & \frac{1}{2} & s\\ \frac{1}{2} & \frac{1}{2} & 1\end{Bmatrix}\\ &+\delta_{jj_1}\,\delta_{mm_1}\,240\pi\,(-)^{j_1+l_1+s_1}\sqrt{\hat{s}\hat{s}_1}\begin{Bmatrix} l_1 & s_1 & j\\ s & l & 2\end{Bmatrix}\begin{Bmatrix} 1 & 1 & 2\\ \frac{1}{2} & \frac{1}{2} & s\\ \frac{1}{2} & \frac{1}{2} & s_1\end{Bmatrix}\\ &\times\sum_{\bar{l}}\hat{\bar{l}}\,H_{\bar{l}}(pp_1)\sum_{a+b=2}\frac{p^a(-p_1)^b}{\sqrt{\hat{a}!\;\hat{b}!}}\begin{Bmatrix} l & l_1 & 2\\ b & a & \bar{l}\end{Bmatrix}\\ &\times C(a0\;\bar{l}0, l0)\,C(b0\;\bar{l}0, l_1 0).\end{aligned} \tag{A.13}$$

Thus the final result for $M_{d_1}^{J,2}$, after evaluating the sums over m and m_1 in Eq. (A.2), becomes

$$\begin{aligned} M_{d_1}^{J,2} = & \frac{\delta(q_1-q)}{q^2}\,\delta_{JJ_1}\,\delta_{MM_1}\,\delta_{jj_1}\,\delta_{\lambda\lambda_1}\,\delta_{II_1} \\ & \times \Bigg[\delta_{ll_1}\,\delta_{ss_1}\,4\pi\,(-)^{s+1}\,\tilde{H}_l(pp_1) \begin{Bmatrix} \frac{1}{2} & \frac{1}{2} & s \\ \frac{1}{2} & \frac{1}{2} & 1 \end{Bmatrix} \\ & + 240\pi\,(-)^{j_1+l_1+s_1}\,\sqrt{\hat{s}\hat{s}_1} \begin{Bmatrix} l_1 & s_1 & j \\ s & l & 2 \end{Bmatrix} \begin{Bmatrix} 1 & 1 & 2 \\ \frac{1}{2} & \frac{1}{2} & s \\ \frac{1}{2} & \frac{1}{2} & s_1 \end{Bmatrix} \\ & \times \sum_{\bar{l}} \hat{\bar{l}}\,H_{\bar{l}}(pp_1) \sum_{a+b=2} \frac{p^a(-p_1)^b}{\sqrt{\hat{a}!\,\hat{b}!}} \begin{Bmatrix} l & l_1 & 2 \\ b & a & \bar{l} \end{Bmatrix} C(a0\,\bar{l}0, l0)\,C(b0\,\bar{l}0, l_10) \Bigg]. \end{aligned} \tag{A.14}$$

A useful test for the correctness of the result (A.14) is a comparison with the result for $M_d^{J,2}$ in ref. [23]. The difference between $M_{d_1}^{J,2}$ and $M_d^{J,2}$ is that the first matrix element has an operator $\boldsymbol{\sigma}_1 \cdot \boldsymbol{Q} = 4\pi\{\sigma_1, Y^1(\hat{Q})\}^{00}$, whereas the latter matrix element has the operator $-i\,\sqrt{2}\,\sqrt{4\pi/3}\,\{\sigma_1, Y^1(\hat{Q})\}^{1\mu}$. Thus the difference between $M_{d_1}^{J,2}$ and $M_d^{J,2}$, besides a different factor in front, is that in one case we have a rank-0 operator and in the other case the same operator, but with rank-1 this time. Of course the replacement of the rank-1 operator in the result for the d-term with the rank-0 operator in order to get the result for the d_1-term is not as straightforward as it might appear and has to be done with great care. Nevertheless, one finds that the result (A.14) for $M_{d_1}^{J,2}$ is consistent with the result (90[23]) for $M_d^{J,2}$.

Besides $M_{d_1}^{J,2}$ we will also need the matrix element

$$M_{d_1}^{J,3} = {}_3\langle p_2 q_2 \alpha_{2J} | \boldsymbol{\sigma}_1 \cdot \boldsymbol{Q}' \;\; \boldsymbol{\sigma}_2 \cdot \boldsymbol{Q}' \, \frac{F(Q'^2)}{Q'^2 + m_\pi^2} \big| p' q' \alpha'_J \big\rangle_3 \tag{A.15}$$

for the first term in Eq. (A.1). $M_{d_1}^{J,3}$ can easily be obtained from $M_{d_1}^{J,2}$ via the symmetry relation

$$M_{d_1}^{J,2}(pq\alpha, p_1 q_1 \alpha_1) = M_{d_1}^{J,3}(p_1 q_1 \alpha_1, pq\alpha). \tag{A.16}$$

The second momentum-spin matrix element occurring in the d_1-term is $\tilde{M}_{d_1}^{J,3}$, Eq. (A.3). For the moment we do not need to specify which choice of Eqs. (13)–(15) we want to make for the short-range operator $\mathcal{O}(Q'^2)$. That means we just use Eq. (46[23]) for the expansion of the angular dependence and do not yet specify how to determine H. With this we get

$$\tilde{M}_{d_1}^{j,3} = 2\pi \sum_{\bar{l}} \sqrt{\hat{\bar{l}}}\,\bar{H}_{\bar{l}}(p'p'_2)\;{}_3\langle p_2 q_2 \alpha_{2J} | \mathscr{Y}_{\bar{l}\bar{l}}^{00}(\hat{p}'\hat{p}_2) \big| p' q' \alpha'_J \big\rangle_3 . \tag{A.17}$$

The matrix element in Eq. (A.16) can easily be evaluated as

$${}_3\langle p_2 q_2 \alpha_{2J} | \mathscr{Y}_{\bar{l}\bar{l}}^{00}(\hat{p}'\hat{p}_2) \big| p' q' \alpha'_J \big\rangle_3 = \delta_{j'j_2}\,\delta_{l'l_2}\,\delta_{s's_2}\,\delta_{m'm_2}\,\frac{(-)^{l'}}{\sqrt{\hat{l}'}} \tag{A.18}$$

and with this we get

$$\tilde{M}_{d_1}^{J,3} = \frac{\delta(q_2 - q')}{q'^2}\;\delta_{J'J_2}\,\delta_{M'M_2}\,\delta_{j'j_2}\,\delta_{l'l_2}\,\delta_{s's_2}\,\delta_{\lambda'\lambda_2}\,\delta_{I'I_2}\,2\pi\,\bar{H}_{l'}(p'p_2). \tag{A.19}$$

The symmetry relation to obtain $\tilde{M}_{d_1}^{J,3}$ is given by

$$\tilde{M}_{d_1}^{J,2}(pq\alpha, p_1 q_1 \alpha_1) = \tilde{M}_{d_1}^{J,3}(p_1 q_1 \alpha_1, pq\alpha)\,. \tag{A.20}$$

Let us now determine $\bar{H}$ for the different choices Eqs. (13)–(15) for $\mathcal{O}(Q^2)$. Choosing $\mathcal{O}(Q^2)$ according to Eq. (13) as a propagator only we get instead of Eqs. (43–44[23])

$$f(x) = \frac{m_{sr}^2}{(\boldsymbol{p}-\boldsymbol{p}_1)^2 + m_{sr}^2} = \frac{m_{sr}^2}{2pp_1}\ \frac{1}{B_{m_{sr}} - x} \tag{A.21}$$

and therefore $\bar{H}$ becomes for this case

$$\bar{H}_l(pp_1) = \frac{m_{sr}^2}{pp_1}\ Q_l(B_{m_{sr}})\,. \tag{A.22}$$

The second case, Eq. (14), where the propagator is multiplied by monopole form factors, has already been calculated in Eqs. (43–47[23]). Thus for this case one has

$$\bar{H}_l(pp_1) = m_{sr}^2 \left\{ \frac{1}{pp_1}\ [Q_l(B_{m_{sr}}) - Q_l(B_{\Lambda_{sr}})] + \frac{\Lambda_{sr}^2 - m_{sr}^2}{2(pp_1)^2}\ Q_l'(B_{\Lambda_{sr}}) \right\}. \tag{A.23}$$

Finally we have the case where the propagator is multiplied by dipole form factors, Eq. (15):

$$\begin{aligned} f(x) &= \frac{m_{sr}^2}{(\boldsymbol{p}-\boldsymbol{p}_1)^2 + m_{sr}^2}\ \left(\frac{\Lambda_{sr}^2}{\Lambda_{sr}^2 + Q^2}\right)^4 \\ &= \frac{m_{sr}^2\,\Lambda_{sr}^8}{(2pp_1)^5} \left\{ \left(\frac{2pp_1}{\Lambda_{sr}^2 - m_{sr}^2}\right)^4 \left[\frac{1}{B_{m_{sr}} - x} - \frac{1}{B_{\Lambda_{sr}} - x}\right] - \left(\frac{2pp_1}{\Lambda_{sr}^2 - m_{sr}^2}\right)^3 \frac{1}{(B_{\Lambda_{sr}} - x)^2} \right. \\ &\quad \left. - \left(\frac{2pp_1}{\Lambda_{sr}^2 - m_{sr}^2}\right)^2 \frac{1}{(B_{\Lambda_{sr}} - x)^3} - \left(\frac{2pp_1}{\Lambda_{sr}^2 - m_{sr}^2}\right) \frac{1}{(B_{\Lambda_{sr}} - x)^4} \right\}. \end{aligned} \tag{A.24}$$

This leads to

$$\begin{aligned} \bar{H}_l(pp_1) = \frac{m_{sr}^2}{(\Lambda_{sr}^2 - m_{sr}^2)^4} &\left\{ \frac{1}{pp_1}\ [Q_l(B_{m_{sr}}) - Q_l(B_{\Lambda_{sr}})] + \frac{\Lambda_{sr}^2 - m_{sr}^2}{2(pp_1)^2}\ Q_l'(B_{\Lambda_{sr}}) \right. \\ &\left. - \frac{(\Lambda_{sr}^2 - m_{sr}^2)^2}{(2pp_1)^2}\ Q_l''(B_{\Lambda_{sr}}) + \frac{(\Lambda_{sr}^2 - m_{sr}^2)^3}{3(2pp_1)^4}\ Q_l'''(B_{\Lambda_{sr}}) \right\}. \end{aligned} \tag{A.25}$$

The only pieces still missing for the PWD of the d_1-term are the isospin matrix elements. They are given by

$$\begin{aligned} I_{d_1} &\equiv {}_2\big\langle (t\tfrac{1}{2}) T M_T | \boldsymbol{\tau}_1 \cdot \boldsymbol{\tau}_2 | (t'\tfrac{1}{2}) T' M_T' \big\rangle_3 \\ &= \delta_{TT'}\,\delta_{M_T M_T'}\,(-6)\,\sqrt{\hat{t}\hat{t}'} \begin{Bmatrix} \frac{1}{2} & \frac{1}{2} & t \\ \frac{1}{2} & T & t' \end{Bmatrix} \begin{Bmatrix} \frac{1}{2} & \frac{1}{2} & t' \\ \frac{1}{2} & \frac{1}{2} & 1 \end{Bmatrix}, \end{aligned} \tag{A.26}$$

$$\begin{aligned} \tilde{I}_{d_1} &\equiv {}_2\big\langle (t\tfrac{1}{2}) T M_T | \boldsymbol{\tau}_3 \cdot \boldsymbol{\tau}_1 | (t'\tfrac{1}{2}) T' M_T' \big\rangle_3 \\ &= \delta_{TT'}\,\delta_{M_T M_T'}\,(-)^{t+t'+1}\,6\,\sqrt{\hat{t}\hat{t}'} \begin{Bmatrix} \frac{1}{2} & \frac{1}{2} & t \\ \frac{1}{2} & T & t' \end{Bmatrix} \begin{Bmatrix} \frac{1}{2} & \frac{1}{2} & t \\ \frac{1}{2} & \frac{1}{2} & 1 \end{Bmatrix} \\ &= \begin{cases} I_{d_1} & \text{for } t = t', \\ -I_{d_1} & \text{for } t \neq t'. \end{cases} \end{aligned} \tag{A.27}$$

Now we can put all parts together in order to obtain the d_1 matrix element. In order to do this we will use an obvious symbolic notation:

$$ {}_1\langle V_4^{(1)}|_{d_1}\rangle_1 = P_{1\leftrightarrow 2}\,\{[\tilde{M}^{J,2}_{d_1}\; P_{2\leftrightarrow 3}\; M^{J,3}_{d_1}]\, I_{d_1} + [M^{J,2}_{d_1}\, P_{2\leftrightarrow 3}\, \tilde{M}^{J,3}_{d_1}]\, \tilde{I}_{d_1}\} P_{3\leftrightarrow 1}. \tag{A.28} $$

A.2 The d_2-Term

The d_2-term is given in Eq. (12) as

$$ \begin{aligned} V_4^{(1)} = &-\frac{d_2}{(2\pi)^6}\,\frac{g_A}{4f_\pi^2}\;\boldsymbol{\sigma}_1\times\boldsymbol{\sigma}_3\cdot\boldsymbol{Q}'\;\;\boldsymbol{\sigma}_2\cdot\boldsymbol{Q}'\;\frac{F(Q'^2)}{Q'^2+m_\pi^2}\;\mathcal{O}_{\rm SR}(Q^2)\;\boldsymbol{\tau}_1\cdot\boldsymbol{\tau}_2\times\boldsymbol{\tau}_3 \\ &-\frac{d_2}{(2\pi)^6}\,\frac{g_A}{4f_\pi^2}\;\mathcal{O}_{\rm SR}(Q'^2)\;\;\boldsymbol{\sigma}_1\times\boldsymbol{\sigma}_2\cdot\boldsymbol{Q}\;\boldsymbol{\sigma}_3\cdot\boldsymbol{Q}\;\frac{F(Q^2)}{Q^2+m_\pi^2}\;\boldsymbol{\tau}_1\cdot\boldsymbol{\tau}_3\times\boldsymbol{\tau}_2\,. \end{aligned} \tag{A.29} $$

The isospin dependence is the same as in the d-term. The isospin matrix element for the d_2-term is therefore already given by Eq. (34[23]): $I_{d_2} = I_d$ and $\tilde{I}_{d_2} = -I_d$.

The d_2-term does not fall into two parts as naturally as the d_1-term does. Nonetheless we can still split it into two quasi-two-body operators by rewriting (for the second term in Eq. (A.29))

$$ \begin{aligned} \boldsymbol{\sigma}_1\times\boldsymbol{\sigma}_2\cdot\boldsymbol{Q} &= i\sqrt{6}\,\sqrt{\frac{4\pi}{3}}\,Q\,\Big\{\{\sigma_1,\sigma_2\}^1, Y^1(\widehat{\boldsymbol{p}'-\boldsymbol{p}_1})\Big\}^{00} \\ &= -i\sqrt{6}\,\sqrt{\frac{4\pi}{3}}\,Q\,\Big\{\sigma_2,\{\sigma_1,Y^1(\hat{Q})\}^1\Big\}^{00} \\ &= i\sqrt{2}\,\sqrt{\frac{4\pi}{3}}\,Q\,\sum_\mu(-)^\mu\sigma_2^\mu\{\sigma_1,Y^1(\hat{Q})\}^{1,-\mu} \end{aligned} \tag{A.30} $$

in analogy to Eq. (77[23]). Therefore we have to calculate the following two matrix elements for the second term of Eq. (A.29):

$$ \begin{aligned} M^{J,2}_{d_2} &= {}_2\langle pq\alpha|i\sqrt{2}\,\sqrt{\frac{4\pi}{3}}\,Q\{\sigma_1,\mathscr{Y}^1_{ab}(\hat{p}\hat{p}_1)\}^{1,-\mu}\,\frac{\boldsymbol{\sigma}_3\cdot\boldsymbol{Q}}{Q^2+m_\pi^2}\;F(Q^2)|\,p_1q_1\alpha_1\rangle_2 \\ &= \frac{\delta(q-q_1)}{q^2}\;\delta_{\lambda\lambda_1}\,\delta_{II_1}\sum_{mm_1}C(jm\;IM-m,JM)\,C(j_1m_1\;I_1M_1-m_1,J_1M_1) \\ &\quad\times\underbrace{{}_2\langle pjm|i\sqrt{2}\,\sqrt{\frac{4\pi}{3}}\,Q\,\{\sigma_1,\mathscr{Y}^1_{ab}(\hat{p}\hat{p}_1)\}^{1,-\mu}\,\frac{\boldsymbol{\sigma}_3\cdot\boldsymbol{Q}}{Q^2+m_\pi^2}\;F(Q^2)|\,p_1j_1m_1\rangle_2}_{\equiv M^{j,2}_{d_2}}\,, \end{aligned} \tag{A.31} $$

$$ \begin{aligned} \tilde{M}^{J,3}_{d_2} &= {}_3\langle p_2q_2\alpha_2|\sigma_2^\mu\,\mathcal{O}(Q')|\,p'q'\alpha'\rangle_3 \\ &= \frac{\delta(q_2-q')}{q'^2}\;\delta_{\lambda'\lambda_2}\,\delta_{I'I_2}\sum_{m'm_2}C(j_2m_2\;I_2M_2-m_2,J_2M_2)\,C(j'm'\;I'M'-m',J'M') \\ &\quad\times\underbrace{{}_3\langle p_2j_2m_2|\sigma_2^\mu\mathcal{O}(Q')|j'j'm'\rangle_3}_{\equiv\tilde{M}^{j,3}_{d_2}}\,. \end{aligned} \tag{A.32} $$

The sum over μ from Eq. (A.30) will be performed later on after we will have put together all the pieces.

The first matrix element, $M_{d_2}^{J,2}$ of Eq. (A.31), occurred already in the d-term (with opposite sign) and is given by Eq. (90[23]):

$$\begin{aligned}
M_{d_2}^{J,2} = & \frac{\delta(q-q_1)}{q^2}\,\delta_{\lambda\lambda_1}\,\delta_{II_1}\,(-)^{I+J}\,\sqrt{\hat{I}\hat{J}j_1\hat{s}\hat{s}_1\hat{J}_1}\;C(1-\mu\;J_1M_1,JM)\begin{Bmatrix}1 & j_1 & j\\ I & J & J_1\end{Bmatrix}\\
& \times\Bigg[\delta_{ll_1}\,i4\pi\sqrt{6}\,(-)^{l+s+1}\,\tilde{H}_l(pp_1)\begin{Bmatrix}l & s & j\\ 1 & j_1 & s_1\end{Bmatrix}\begin{Bmatrix}1 & 1 & 1\\ \frac{1}{2} & \frac{1}{2} & s_1\\ \frac{1}{2} & \frac{1}{2} & s\end{Bmatrix}\\
& +i240\pi\sqrt{6}\,(-)^{j_1}\sum_{\bar{l}}\hat{\bar{l}}\,H_{\bar{l}}(pp_1)\sum_{a+b=2}\frac{p^a\;p_1^b}{\sqrt{(2a)!\,(2b)!}}\\
& \times\begin{Bmatrix}a & b & 2\\ l_1 & l & \bar{l}\end{Bmatrix}C(a0\;\bar{l}0,l0)\;C(b0\;\bar{l}0,l_1 0)\\
& \times\sum_{i_1}\hat{i}_1\begin{Bmatrix}2 & i_1 & 1\\ 1 & 1 & 1\end{Bmatrix}\begin{Bmatrix}2 & i_1 & 1\\ l_1 & s_1 & j_1\\ l & s & j\end{Bmatrix}\begin{Bmatrix}1 & 1 & i_1\\ \frac{1}{2} & \frac{1}{2} & s_1\\ \frac{1}{2} & \frac{1}{2} & s\end{Bmatrix}\Bigg]\\
= & -M_d^{J,2}.
\end{aligned}\tag{A.33}$$

(Note that there are two misprints in Eq. (90[23]): The phase in the second line of Eq. (90[23]) must read $(-)^{l+s+1}$, and the phase $(-)^i$ in the third line has to be eliminated.)

For the first term in Eq. (A.29) we need

$$\begin{aligned}
\boldsymbol{\sigma}_1\times\boldsymbol{\sigma}_3\cdot\boldsymbol{Q}' &= i\sqrt{6}\,\sqrt{\frac{4\pi}{3}}\,Q'\Big\{\{\sigma_1,\sigma_3\}^1,Y^1(\widehat{\boldsymbol{p}'-\boldsymbol{p}_2})\Big\}^{00}\\
&= -i\sqrt{6}\,\sqrt{\frac{4\pi}{3}}\,Q'\Big\{\sigma_3,\{\sigma_1,Y^1\hat{Q}'\}^1\Big\}^{00}\\
&= i\sqrt{2}\,\sqrt{\frac{4\pi}{3}}Q'\;\sum_{\mu}(-)^{\mu}\sigma_3^{\mu}\{\sigma_1,Y^1(\hat{Q}')\}^{1,-\mu},
\end{aligned}\tag{A.34}$$

which leads us to calculate the matrix element

$$M_{d_2}^{J,3} = {}_3\langle p_2q_2\alpha_2|i\sqrt{2}\,\sqrt{\frac{4\pi}{3}}\,Q'\{\sigma_1,\mathscr{Y}^1_{ab}(\hat{p}'\hat{p}_2)\}^{1,-\mu}\,\frac{\boldsymbol{\sigma}_2\cdot\boldsymbol{Q}'}{Q'^2+m_\pi^2}\;F(Q'^2)|p'q'\alpha'\rangle_3\tag{A.35}$$

and $M_{d_2}^{J,3} = -M_d^{J,3}$. Eq. (91[23]) gives $M_{d_2}^{J,3}$ and Eqs. (92–93[23]) the relation between $M_{d_2}^{J,2}$ and $M_{d_2}^{J,3}$. Note that Eq. (93[23]) has a misprint in the phase; the correct phase must be $(-)^{s+s_1}$.

For the second matrix element, $\tilde{M}_{d_2}^{J,3}$ in Eq. (A.32), we need

$$\begin{aligned}
\tilde{M}_{d_2}^{j,3} = & \frac{\delta(p_2-p')}{p'^2}\;\delta_{l_2l'}\,C(1\mu\;j'm',j_2m_2)\sqrt{6}\;2\pi\bar{H}_{l'}(p_2p')\\
& \times(-)^{j'+l'+s'+s_2}\,\sqrt{\hat{j}'\hat{s}'\hat{s}_2}\begin{Bmatrix}s' & j' & l'\\ j_2 & s_2 & 1\end{Bmatrix}\begin{Bmatrix}\frac{1}{2} & \frac{1}{2} & s'\\ 1 & s_2 & \frac{1}{2}\end{Bmatrix}.
\end{aligned}\tag{A.36}$$

Again, what we have to insert for $\bar{H}$ depends on our choice for $\mathscr{O}$.

With Eq. (A.36) we get after performing the sums over m_2 and m' in Eq. (A.32)

$$\begin{aligned}\tilde{M}^{J,3}_{d_2} = &\frac{\delta(p_2-p')}{p'^2}\,\frac{\delta(q_2-q')}{q'^2}\,\delta_{l_2l'}\,\delta_{\lambda_2\lambda'}\,\delta_{I_2I'}\,\sqrt{6}\,2\pi\bar{H}_{l'}(p_2p') \\ &\times(-)^{1+I'+s'+s_2+I'+J_2}\sqrt{\hat{j}'\hat{j}_2\hat{s}'\hat{s}_2\hat{J}_2}\begin{Bmatrix} s' & j' & l' \\ j_2 & s_2 & 1\end{Bmatrix}\begin{Bmatrix}\frac{1}{2} & \frac{1}{2} & s' \\ 1 & s_2 & \frac{1}{2}\end{Bmatrix} \\ &\times\begin{Bmatrix}1 & j' & j_2 \\ I' & J_2 & J'\end{Bmatrix} C(1\mu\; J'M', J_2M_2). \end{aligned} \tag{A.37}$$

Similarly we get

$$\begin{aligned}\tilde{M}^{J,2}_{d_2} = &\frac{\delta(p-p_1)}{p^2}\,\frac{\delta(q-q_1)}{q^2}\,\delta_{ll_1}\,\delta_{\lambda\lambda_1}\,\delta_{II_1}\,\sqrt{6}\,2\pi\bar{H}_l(pp_1) \\ &\times(-)^{1+l+I+J}\sqrt{\hat{j}\hat{j}_1\hat{s}\hat{s}_1\hat{J}_1}\begin{Bmatrix} s & j & l \\ j_1 & s_1 & 1\end{Bmatrix}\begin{Bmatrix}\frac{1}{2} & \frac{1}{2} & s \\ 1 & s_1 & \frac{1}{2}\end{Bmatrix} \\ &\times\begin{Bmatrix}1 & j & j_1 \\ I & J_1 & J\end{Bmatrix} C(1\mu\; J_1M_1, JM). \end{aligned} \tag{A.38}$$

References

1. Witała, H., Kamada, H., Nogga, A., Glöckle, W., Elster, Ch., Hüber, D.: Phys. Rev. **C59**, 3035 (1999); Abfalterer, W. P., et al.: Phys. Rev. Lett. **81**, 57 (1998)
2. Witała, H., Glöckle, W., Hüber, D., Golak, J., Kamada, H.: Phys. Rev. Lett. **81**, 1183 (1998); Rohdjess, H., et al.: Phys. Rev. **C57**, 2111 (1998)
3. Glöckle, W., Witała, H., Hüber, D., Kamada, H., Golak, J.: Phys. Rep. **274**, 107 (1996)
4. Hüber, D., Friar, J. L.: Phys. Rev. **C58**, 674 (1998)
5. Fujita, J.-I., Miyazawa, H.: Prog. Theor. Phys. **17**, 360 (1957)
6. Coon, S. A., Scadron, M. D., McNamee, P. C., Barrett, B. R., Blatt, D. W. E., McKellar, B. H. J.: Nucl. Phys. **A317**, 242 (1979); Coon, S. A., Glöckle, W.: Phys. Rev. **C23**, 1790 (1981)
7. Coelho, H. T., Das, T. K., Robilotta, M. R.: Phys. Rev. **C28**, 1812 (1983); Robilotta, M. R., Coelho, H. T.: Nucl. Phys. **A460**, 645 (1986)
8. Carlson, J., Pandharipande, V. R., Wiringa, R. B.: Nucl. Phys. **A401**, 59 (1983)
9. van Kolck, U.: Thesis. University of Texas 1993; Ordóñez, C., van Kolck, U.: Phys. Lett. **B291**, 459 (1992); van Kolck, U.: Phys. Rev. **C49**, 2932 (1994)
10. Eden, J. A., Gari, M. F.: Phys. Rev. **C53**, 1510 (1996); Eden, J. A.: Private communication
11. Friar, J. L., Hüber, D., van Kolck, U.: Phys. Rev. **C59**, 53 (1999)
12. Friar, J. L., Gibson, B. F., Payne, G. L., Coon, S. A.: Few-Body Systems **5**, 13 (1988)
13. Nogga, A., Hüber, D., Kamada, H., Glöckle, W.: Phys. Lett. **B409**, 19 (1997)
14. Hüber, D.: Private communication
15. Wiringa, R. B., Stoks, V. G. J., Schiavilla, R.: Phys. Rev. **C51**, 38 (1995)
16. Ellis, R. G., Coon, S. A., McKellar, B. H. J.: Nucl. Phys. **A438**, 631 (1985)
17. McKellar, B. H. J.: Lecture Notes in Physics **260**, 7 (1986); Coon, S. A.: Lecture Notes in Physics **260**, 92 (1986); Coon, S. A.: Few-Body Systems, Suppl. **1**, 41 (1986); Coon, S. A., Peña, M. T.: Phys. Rev. **C48**, 2559 (1993)
18. Witała, H., Hüber, D., Glöckle, W., Golak, J., Stadler, A., Adam Jr., J.: Phys. Rev. **C52**, 1254 (1995)
19. Coon, S. A., Peña, M. T., Riska, D. O.: Phys. Rev. **C52**, 2925 (1995)
20. Hüber, D., Witała, H., Glöckle, W.: Few-Body Systems **14**, 171 (1993)
21. Hüber, D., Kamada, H., Witała, H., Glöckle, W.: Acta Phys. Pol. **B28**, 1677 (1997)

22. Glöckle, W.: The Quantum Mechanical Few-Body Problem, pp. 132–137. Berlin-Heidelberg-New York: Springer 1983. This comprehensive examination of the three-nucleon problem has an extensive discussion of permutations
23. Hüber, D., Witała, H., Nogga, A., Glöckle, W., Kamada, H.: Few-Body Systems **22**, 107 (1997)
24. Hüber, D.: PhD Thesis. Bochum 1993 (unpublished)
25. McAninch, J. E., Haeberli, W., Witała, H., Glöckle, W., Golak, J.: Phys. Lett. **B307**, 13 (1993); McAninch, J. E., Lamm, L. O., Haeberli, W.: Phys. Rev. **C50**, 589 (1994)
26. Howell, C. R., et al.: Few-Body Systems **2**, 19 (1987)
27. Romero, J. L., et al.: Phys. Rev. **C25**, 2214 (1982); Watson, J. W., et al.: Phys. Rev. **C25**, 2219 (1982)
28. Coon, S. A., Friar, J. L.: Phys. Rev. **C34**, 1060 (1986). Eq. (33b) should equal Eq. (27b), but contains a typographical error: The indices i and j should be interchanged in Eq. (33b) [Adam, J.: Private communication]

Received September 16, 1999; accepted for publication October 20, 1999